MDPI

Article

Mitigating Intermittency in Offshore Wind Power Using Adaptive Nonlinear MPPT Control Techniques

Muhammad Waqas Ayub[1], Inam Ullah Khan[2], George Aggidis[1], and Xiandong Ma[1]*

† Correspondence: xiandong.ma@lancaster.ac.uk
‡ Current address: Lancaster University, UK

Abstract: This paper addresses the challenge of maximizing power extraction in offshore wind energy systems through the development of an enhanced Maximum Power Point Tracking (MPPT) control strategy. Offshore wind energy is inherently intermittent, leading to discrepancies between power generation and electricity demand. To address this issue, we propose three advanced control algorithms to do comaprative analysis: Sliding Mode Control (SMC), Integral Back-Stepping-Based Real-Twisting Algorithm (IBRTA), and Feed-Back Linearization (FBL). These algorithms are designed to handle the nonlinear dynamics and aerodynamic uncertainties associated with offshore wind turbines. Given the practical lim- itations in acquiring accurate nonlinear terms and aerodynamic forces, our approach focuses on ensuring the adaptability and robustness of the control algorithms under varying operational conditions. The proposed strategies are rigorously evaluated through MATLAB/Simulink simulations across multiple wind speed scenarios. Comparative analysis demonstrates the superior performance of the proposed methods in optimizing power extraction under diverse conditions, contributing to the advance- ment of MPPT techniques for offshore wind energy systems.

Keywords: Offshore Wind Energy, Sliding Mode Control, Nonlinear Control Algorithms, Aerodynamic Uncertainties

1. Introduction

Renewable energy sources now make up nearly a third of global electricity production, driven by the increasing demand for clean, sustainable energy solutions and the continuous advancement of renewable technologies. Wind energy, in particular, has emerged as a leading contributor to this transition, with global wind capacity reaching over 837 GW by 2022, accounting for nearly 7% of global electricity generation [1]. Offshore wind energy systems are at the forefront of this growth, offering the potential to generate up to 40% more power than onshore installations due to higher and more consistent wind speeds [2]. However, the efficiency of offshore wind systems is highly contingent on the ability to optimize power extraction in the face of variable and unpredictable wind conditions.

The MPPT control schemes are very important for the effective control of offshore wind turbines to ensure that they produce their maximum power output [3]. Most of the traditional MPPT techniques, though successful to some extent, fail to cope up with the fluctuating and non-linear behavior of offshore wind systems. Variable speed turbines (VST) which have the capability of varying their rotational speed depending on the wind speed are more efficient than the fixed speed turbines (FST) with a potential of up to 10-15% increase in energy generation [4], [5]. However, the application of efficient MPPT techniques in offshore systems continues to be a challenge, especially in dealing with issues arising from nonlinearities and disturbances in the environment [6], [7].

To address these challenges, new developments in control theory and artificial intelligence have provided new opportunities to improve MPPT in offshore wind energy systems. Some of the methods used include sliding mode control (SMC), integral backstepping,

Citation: Mitigating Intermittency in Offshore Wind Power Using Adaptive Nonlinear MPPT Control Techniques. *Journal Not Specified* **2024**, *1*, 0. h...ttpdoi.org/

Received: March, 2024
Accepted: xxxxx
Published: Energies

and super-twisting algorithm (STA), which are deemed to improve conventional methods [8]. These methods are intended to be insensitive to the variations of parameters and the disturbances that act in the offshore environment that is rough and uncertain. More specifically, the application of artificial intelligence including fuzzy logic control (FLC) and neural networks has also been incorporated to improve the flexibility of these control systems. The offshore wind will increase its capacity at a rate of more than 15% every year over the next ten years, which underlines the importance of improving the state-of-the-art MPPT control strategies to optimize the potential of offshore wind energy sources [9]. The enhancement of power capture in wind energy systems has been a major concern, especially in modern and increasingly installed offshore wind farms. Some of the first techniques used for MPPT were perturb and observe (P&O) and incremental conductance [10]. Although these methods are simple and commonly used, they have a major weakness in handling the dynamic and stochastic nature of offshore wind conditions. The above-mentioned conventional MPPT techniques have been reported to produce poor performance under turbulent wind conditions, which in turn cause energy losses [11], [12].

In order to overcome these draw backs, enhanced control techniques have been proposed in the literature for enhancing the efficiency of MPPT techniques. As a consequence, SMC is considered an effective approach owing to its ability to handle parameters variability and disturbance [13]. The above features make SMC suitable for use in offshore environments since it is capable of retaining stability even in different circumstances. However, conventional SMC methods are known to produce chattering, which is a condition that causes mechanical wear and decreases system performance. Some developments in SMC has been made recently for instance the IBRTA to overcome such problems while at the same time giving the system a robust control response.

AI based MPPT techniques have been enhanced by integrating AI into the wind energy control system. FLC has been employed extensively due to its capability to deal with nonlinearity and uncertainty without calling for an accurate model of the system [14]. FLC systems are more efficient in tracking the stochastic nature of wind and provide faster tracking of the MPP than the conventional methods. Furthermore, the use of Neural Networks (NNs) has also been adopted to predict the wind speed and to enhance the turbine efficiency in the data driven manner [15]. These AI-based techniques improve the flexibility of the MPPT systems which make it easier to control the systems in dynamic offshore conditions.In [16], gave a comprehensive review of MPPT methods specifically for PMSG-based wind energy systems ranging from traditional hill-climbing and perturb-and-observe to sophisticated AI-assisted algorithms.

In generator technologies, PMSG has been used in wind energy because of the high efficiency and reliability of the system [16]. Some of the advantages of PMSGs include; low maintenance cost and no power loss through the gear box. This is because PMSGs produce higher efficiency and are long lasting when used with other complex MPPT techniques [16]. The studies have also shown that the use of PMSG in variable speed wind turbines and appropriate control techniques improve the power output and the reliability of the system in the face of varying wind gusts [11], [17].

However, there is a problem in the area of the MPPT in offshore wind energy systems which has been a topic of discussion. Future work should focus on the advanced control approaches like Observer-based control techniques like IBSMC [18]. These methods are intended to enhance the efficiency and reliability of MPPT systems especially in the dynamic conditions of the offshore wind conditions [19]. There is the detailed analysis of both wind-wave sources combining the observer-based techniques with the artificial intelligence techniques, researchers are striving to design the more robust and effective control systems which can optimally utilize the offshore wind energy resources.

2. SYSTEM MODELLING

In this section, we develop the mathematical models for the offshore wind energy conversion system and the PMSG. These models are foundational for the design of ad-

vanced control strategies that will be discussed in subsequent sections. An offshore wind conversion's typical layout is shown in Fig. 1.

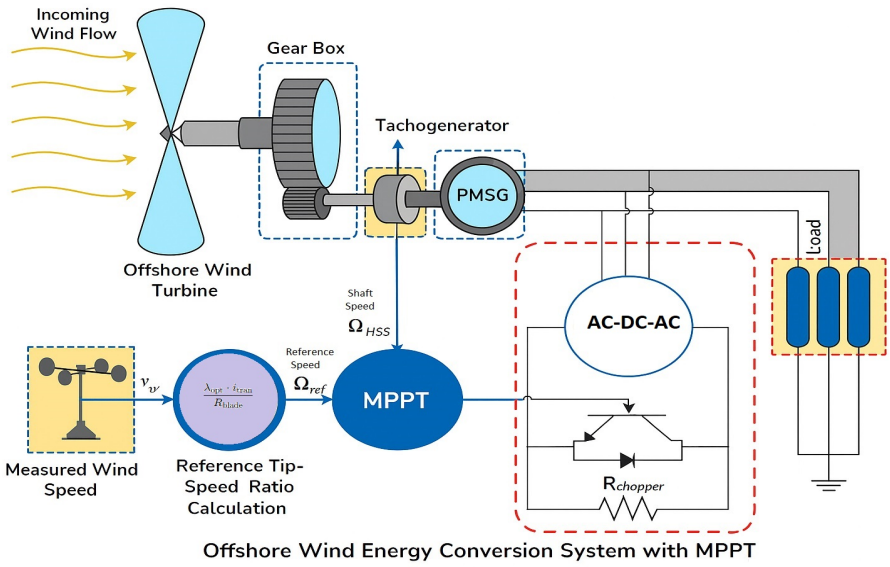

Figure 1. Schematic diagram of the complete variable speed PMSG-based WECS

The primary objective of this section is to model the energy conversion process of an offshore wind turbine and its associated generator, the PMSG. The modeling will encompass both mechanical and electrical dynamics, leading to a state-space representation suitable for control design.

2.0.1. Power and Torque Calculations

The amount of electricity that an offshore wind turbine is capable of producing is influenced by a number of factors such as the wind speed, the density of the air and the dimensions of the turbine. The mechanical power output P_{M} of an offshore wind system can be calculated as [13]:

$$P_{\mathrm{M}} = \frac{1}{2}\rho_{\mathrm{air}}\pi R_{\mathrm{blade}}^{2} v_{\mathrm{wind}}^{3} C_{\mathrm{pr}}(\lambda_l) \tag{1}$$

where ρ_{air} is the air density, R_{blade} is the radius of the turbine blade, v_{wind} is the wind speed, and $C_{\mathrm{pr}}(\lambda_l)$ is the power coefficient, which is a function of the tip-speed ratio λ_l. The torque exerted on the turbine shaft Γ_{M} is another critical parameter and is calculated using the torque coefficient $C_{\tau}(\lambda_l)$, that is linked to the power coefficient through the following equation:

$$\Gamma_{\mathrm{M}} = \frac{1}{2}\rho_{\mathrm{air}}\pi R_{\mathrm{blade}}^{3} v_{\mathrm{wind}}^{2} C_{\tau}(\lambda_l) \tag{2}$$

The equations provided serve as the groundwork for understanding how mechanical energy is converted in offshore wind turbines. The power coefficient $C_{\mathrm{pr}}(\lambda_l)$ and torque coefficient $C_{\tau}(\lambda_l)$ depends on the tip-speed ratio which is very important in deciding the efficiency of energy conversion.

2.0.2. The Role of Tip-Speed Ratio in Determining Power Output

The tip-speed ratio λ_l is a critical factor in determining the efficiency of power conversion and is defined as:

$$\lambda_l = \frac{\Omega_{\mathrm{HS}} R_{\mathrm{blade}}}{v_{\mathrm{wind}} i_{\mathrm{trans}}} \tag{3}$$

In this context, Ω_{HS} refers to the angular speed of the high-speed shaft, while i_{trans} is the transmission ratio explained earlier in the theoretical background. The power coefficient

Table 1. Constant PMSG terms

Parameter	Value	Parameter	Value
ψ_1	26.147	ψ_4	26.147
ψ_2	0.94866	ψ_5	3.000
ψ_3	8.2264	ψ_6	1.3146
ψ_8	9.945	ψ_9	0.1332
ψ_{10}	0.00506	ψ_{11}	23.806

$C_{\text{pr}}(\lambda_l)$ can be expressed as a polynomial function of λ_l to reflect the complex relationship between wind speed and the rotational speed of the turbine:

$$C_{\text{pr}}(\lambda_l) = -\lambda_l(-0.00610 + 0.0013\lambda_l - 0.0081\lambda_l^2 + 0.00097477\lambda_l^3) \tag{4}$$

The torque coefficient $C_\tau(\lambda_l)$ is found by taking the ratio of the power coefficient to the tip-speed ratio:

$$C_\tau(\lambda_l) = \frac{C_{\text{pr}}(\lambda_l)}{\lambda_l} \tag{5}$$

These relationships are useful in underlining the need of controlling the tip speed ratio in order to enhance the effectiveness of energy conversion in offshore wind systems.

*2.1. **PMSG System***

2.1.1. dq-Axis Representation

Offshore wind turbines employ the PMSG which owns the electrical characteristics described in the $dq-axis$ reference frame The dynamic behavior of the PMSG can be described by the following differential equations [16], [17]:

$$\begin{aligned}
\dot{i_d} &= \frac{-R_{\text{stator}} i_d + p_{\text{pole}}(L_q - L_{\text{chopper}})\Omega_{\text{HS}} i_q - R_{\text{chopper}} i_d}{(L_d + L_{\text{chopper}})} \\
\dot{i_q} &= \frac{-R_{\text{stator}} i_q - p_{\text{pole}}(L_q + L_{\text{chopper}})\Omega_{\text{HS}} i_d - R_{\text{chopper}} i_q}{(L_q + L_{\text{chopper}})} + p_{\text{pole}}\Omega_{\text{HS}}\phi_{\text{constant}} \\
\dot{\Omega}_{\text{HS}} &= \frac{1}{J_{\text{HS}}}\left[-p_{\text{pole}}\phi_{\text{constant}} i_q + \frac{d_1 v_{\text{wind}}^2}{i_{\text{trans}}} + \frac{d_2 v_{\text{wind}}\Omega_{\text{HS}}}{i_{\text{trans}}^2} + \frac{d_3\Omega_{\text{HS}}^2}{i_{\text{trans}}^3}\right]
\end{aligned} \tag{6}$$

In these equations, i_d and i_q denote the dq-axis currents; R_{stator} is the stator resistance; L_d and L_q are the inductances along the d- and q-axes, respectively; ϕ_{constant} represents the flux linkage constant; Ω_{HS} is the angular velocity of the high-speed shaft; and J_{HS} is its moment of inertia. Together, these expressions form a detailed dynamic model of the PMSG system, which is crucial for developing effective control strategies for MPPT in offshore wind energy applications.

2.1.2. State-Space Representation

To streamline the control design process, the PMSG system is expressed in a state-space form. By introducing the state variables $x_1 = i_d$, $x_2 = i_q$, and $x_3 = \Omega_{\text{HS}}$, the dynamic behavior of the system can be represented in a more compact form as follows [**?**]:

$$\dot{x} = f(x) + g(x)u + \Delta(x,t) \tag{7}$$

where $x = [x_1, x_2, x_3]^T$ is the state vector, u is the control input (e.g., R_{chopper}), and $\Delta(x,t)$ represents matched uncertainties in the system. The values of the constants ψ_1 to ψ_{11} in the state-space model are specified in Table 1.

This state-space representation will be used in the subsequent sections to design advanced control strategies that ensure the efficient and stable operation of the offshore wind energy system.

*2.2. **Normal Form Conversion***

2.2.1. Transformation Process

To simplify the control design, the wind conversion model can be transformed into its normal form. The system is represented as:

$$\dot{x} = f(x) + g(x)u + \Delta(x,t), \quad y = h(x) = x_3 \tag{8}$$

where y represents the system output (e.g., Ω_{HS}). The normal form transformation facilitates the design of controllers by separating the internal and external dynamics of the system.

2.2.2. Zero Dynamics and Stability

Zero dynamics refer to the internal behavior of a system when its output is forced to remain at zero. The system's overall stability depends heavily on these zero dynamics being stable. They are determined by applying the conditions $z_1 = z_2 = u = 0$ in the transformed equations:

$$\dot{z}_3 = -z_3(\Gamma_1 - \alpha_1) \tag{9}$$

Stability is maintained when $\Gamma_1 > \alpha_1$, ensuring that the internal dynamics do not destabilize the system.

3. PROPOSED CONTROL SCHEME FOR MPPT

In this section, we present a detailed approach for optimizing power extraction from offshore wind turbines using MPPT techniques. The proposed control scheme aims to operate the wind energy conversion system at its MPP by implementing advanced control strategies. The selected control methods FBL, SMC, and the new IBRTA represent the following alternate nonlinear control paradigms: model-based linearization, discontinuous robust design, and adaptive higher-order feedback, respectively. This selection enables critical performance comparison under typical offshore wind variability. The new IBRTA controller was designed to minimize chattering observed in SMC while maintaining its disturbance rejection capability.

*3.1. **Sliding Mode Control Design***

SMC is a powerful control technique known for its robustness against system uncertainties and external disturbances. SMC achieves control objectives by enforcing the system trajectories to follow a sliding surface, defined in the state space, where the system exhibits desired behavior. The key advantage of SMC is its ability to maintain stability and performance even in the presence of model inaccuracies and external perturbations.

3.1.1. Definition of Sliding Surface

The initial stage in designing a sliding mode controller involves specifying a sliding surface $s(x)$ that characterizes the desired behavior of the system. This surface is generally formulated based on the tracking error $e(t)$, which quantifies the deviation between the reference signal (desired state) and the actual system state:

$$s(x) = \mu_1 e(t) + \dot{e}(t) + \mu_2 \int_0^t e(t)\, dt \tag{10}$$

where μ_1 and μ_2 are positive constants that shape the sliding surface, and $e(t)$ is the tracking error:

$$e(t) = z_1 - z_{\text{reference}}(t) \tag{11}$$

Here, z_1 represents the system state corresponding to the angular velocity of the high-speed shaft (Ω_{HS}), and $z_{\text{reference}}(t)$ is the desired reference value for Ω_{HS}.

3.1.2. Control Law Design

SMC law is formulated to steer the system trajectories toward a designated sliding surface and to retain them on that surface. The total control input is expressed as:

$$u(t) = u_{\text{equivalent}}(t) + u_{\text{discontinuous}}(t)$$

where:

- $u_{\text{equivalent}}(t)$ maintains the system motion on the sliding surface once it has been reached,
- $u_{\text{discontinuous}}(t)$ drives the system trajectories toward the sliding surface from arbitrary initial conditions.

$$u(t) = u_{\text{equivalent}}(t) + u_{\text{discontinuous}}(t) \tag{12}$$

The equivalent control input is responsible for stabilizing the system along the sliding surface:

$$u_{\text{equivalent}}(t) = \frac{1}{L_g L_f h(x)} (\ddot{z}_{\text{reference}} - \ell_1 z_2 - \ell_2 z_1 + \ell_1 \dot{z}_{\text{reference}} + \ell_2 z_{\text{reference}} - {L_f}^2 h(x)) \tag{13}$$

The discontinuous control input is designed to ensure that the system reaches the sliding surface quickly:

$$u_{\text{discontinuous}}(t) = -\ell_3 s(x) - \ell_4 \,\text{sign}(s(x)) \tag{14}$$

where ℓ_1, ℓ_2, ℓ_3, and ℓ_4 are positive gains that are tuned to achieve the desired closed-loop system performance.

3.1.3. Stability Analysis

The stability of the closed-loop system using SMC can be established by analyzing the time derivative of a Lyapunov candidate function $V(s)$, defined as:

$$V(s) = \frac{1}{2} s(x)^2 \tag{15}$$

The time derivative of $V(s)$ along the system trajectories is given by:

$$\dot{V}(s) = s(x)\dot{s}(x) \tag{16}$$

Substituting the control law into the derivative, we obtain:

$$\dot{V}(s) = -\ell_3 s(x)^2 - \ell_4 |s(x)| \tag{17}$$

Since $\ell_3 > 0$ and $\ell_4 > 0$, it follows that $\dot{V}(s) \leq 0$, ensuring that the system trajectories converge to the sliding surface and remain there, thereby guaranteeing the stability of the system.

3.1.4. Mitigating Chattering with Higher-Order Sliding Modes

Chattering is a common issue in SMC, where high-frequency oscillations occur due to the discontinuous control input. To mitigate this effect, we employ Higher-Order Sliding Mode (HOSM) techniques, such as the IBRTA. HOSM reduces chattering by smoothing the control action, leading to improved system performance and reduced wear on mechanical components.To further reduce chattering in SMC, especially when acting under high-frequency disturbances, a few complementary methods can be incorporated in the

design of the control. A popular way around is to introduce a saturation function in a given boundary layer, where the discontinuous sign function is substituted by a smooth approximation. This relaxes the control action in the vicinity of the sliding surface and hence minimizes high-frequency switching. Also, adaptive gain tuning is able to make the control gain adaptive in real-time based upon the tracking error, to provide sufficient control effort without necessarily aggressive switching. An observer-based SMC structure can be utilized to reduce the effects of disturbances in a better way. This enables estimation and cancellation of the disturbances prior to their effect on the system output which enhances robustness. Furthermore, second-order sliding mode algorithms (like the super-twisting algorithm, which is partially incorporated in the IBRTA controller already) improve on the chattering mitigation further by avoiding direct differentiation of the sliding variable. Lastly, unmodeled dynamics or delays can be estimated and corrected using time-delay estimation (TDE) based methods to keep the performance high whilst preventing the sudden transitions in control that can cause chattering. Together, these techniques can preserve the fundamental strength of SMC and at the same time dampen objectionable vibrations in realistic applications.

Algorithm 1 Improved Backstepping Robust Twisting Algorithm (IBRTA) for MPPT

Initialization:
Set system parameters: air density ρ_{air}, blade radius R_{blade}, etc.
Set initial conditions: initial angular speed $\Omega_{\text{HS}}(0)$, wind speed $v_{\text{wind}}(0)$.
Define control gains: ℓ_1, ℓ_2, ℓ_3, ℓ_4, ℓ_8, ℓ_9, etc.
Set desired tip-speed ratio λ_{opt} and power coefficient $C_{\text{pr,max}}$.
Loop: For each time step t during the simulation
Measure the current wind speed $v_{\text{wind}}(t)$.
Calculate the actual tip-speed ratio $\lambda(t) = \frac{\Omega_{\text{HS}}(t) \cdot R_{\text{blade}}}{v_{\text{wind}}(t)}$.
Calculate the desired angular speed $\Omega_{\text{ref}}(t)$ using λ_{opt}.
Calculate the tracking error $er(t) = \Omega_{\text{ref}}(t) - \Omega_{\text{HS}}(t)$.
Step 2: Apply IBRTA Control Law
Compute the error derivative $\dot{er}(t)$.
Update the sliding surface: $s(t) = \ell_1 \cdot er(t) + \ell_2 \cdot \dot{er}(t) + \ell_3 \int_0^t er(\tau) d\tau$.
Compute the equivalent control input $u_{\text{equiv}}(t)$.
Compute the discontinuous control input $u_{\text{discon}}(t) = -\ell_9 \cdot s(t) - \ell_{10} \cdot \text{sign}(s(t))$.
Apply the total control input $u(t) = u_{\text{equiv}}(t) + u_{\text{discon}}(t)$.
Step 3: Update system state
Apply the control input $u(t)$ to the system.
Step 4: Check for convergence
If the tracking error $|er(t)|$ is within the acceptable range, proceed with normal operation.
End Loop
Continue until the end of the simulation time T_{sim}.
Output: Final values of angular speed, power output, and other performance metrics.

3.2. Design of MPPT Control Strategy Based On IBRTA

The IBRTA is an advanced control strategy designed to overcome the limitations of traditional SMC, particularly the chattering phenomenon. IBRTA combines the robustness of SMC with the smooth control action of backstepping and twisting algorithms, resulting in enhanced tracking performance and reduced chattering.

3.2.1. Design of the IBRTA Control Law

The IBRTA control law is composed of an ideal control input $u_{\text{ideal}}(t)$ and a discontinuous control input $u_{\text{discontinuous}}(t)$:

$$u(t) = u_{\text{ideal}}(t) + u_{\text{discontinuous}}(t) \tag{18}$$

The ideal control input is designed using a backstepping approach:

$$u_{\text{ideal}}(t) = -\ell_5 er_1 - \ell_6 er_2 \tag{19}$$

where ℓ_5 and ℓ_6 are positive gains, and $er_1 = e(t)$ and $er_2 = \dot{e}(t)$ are the tracking errors. The discontinuous control input is designed to ensure robustness against disturbances and uncertainties:

$$u_{\text{discontinuous}}(t) = \frac{-1}{L_g L_f h(x)} \left({L_f}^2 h(x) + \ell_8 \dot{er}_1 + \ell_9 s_1 + \ell_{10} \operatorname{sign}(s_1) \right) \tag{20}$$

where ℓ_8, ℓ_9, and ℓ_{10} are positive gains that are tuned to optimize the control performance.

3.2.2. Lyapunov Stability and Convergence Analysis

The stability of the IBRTA control law is analyzed using a composite Lyapunov function $V_2(er_1, s_1)$, defined as:

$$V_2(er_1, s_1) = \frac{1}{2} \left(er_1^2 + s_1^2 \right) \tag{21}$$

Taking the time derivative of V_2 and substituting the control law, we obtain:

$$\dot{V}_2 = -\ell_8 er_1^2 - \ell_9 s_1^2 - \ell_{10} |s_1| \tag{22}$$

Since all gains are positive, $\dot{V}_2 \leq 0$, ensuring that the system is globally asymptotically stable and that the tracking error converges to zero.

3.2.3. Control Gains

The control gains used in the SMC and IBRTA are provided in Table 3. These gains are tuned to achieve the desired closed-loop performance, ensuring robustness and stability under varying wind conditions.

3.2.4. Inverter Model and Power Conversion

A VSI unit serves as a power electronic component to control the output voltage and current. The model of an inverter behaves as follows:

$$V_d c = V_i n - I_d c R_f - L_f * (\frac{I_d c}{I_d t}) \tag{23}$$

where $V_d c$ is the DC-link voltage, $V_i n$ is the input voltage from the generator, $I_d c$ is the DC-link current, and $R_f - L_f$ are the filter resistance and inductance.

Table 2. Key parameters of the system components

Component	Parameter	Value
Wind Turbine	Air Density, ρ_{air}	1.2500 kg/m^3
	Radius of Blades, R_{blade}	2.5000 m
	Optimal Tip-Speed Ratio, λ_{lopt}	7.000
	Transmission Gear Ratio, i_{trans}	7.000
	Maximum Power Coefficient, $C_{pr_{max}}$	0.476
	Mean Wind Velocity, v_{wind}	7.000 m/s
PMSG	Stator Resistance, R_{stator}	3.300 Ω
	Inductance of Load, $L_{chopper}$	0.00800 H
	Flux Linkage Constant, $\phi_{constant}$	438.200 mWb
	Number of Pole Pairs, p_{pole}	3

Table 3. Parameters used in control algorithms

Control Method	Parameter	Value
SMC	Gain 1, ℓ_1	103
	Gain 2, ℓ_2	2000
	Gain 3, ℓ_3	0.01
	Gain 4, ℓ_4	50
IBRTA	Gain 1, ℓ_8	0.1
	Gain 2, ℓ_9	100
	Gain 3, ℓ_{10}	0.001
	Gain 4, ℓ_{12}	2
	Gain 5, ℓ_{11}	700

4. SIMULATION RESULTS AND DISCUSSIONS

This section presents the simulation results of the proposed control strategies, evaluating their performance under two distinct scenarios: a stochastic wind speed profile and a deterministic offshore wind speed profile. The performance of the IBRTA, SMC, and FBL controllers is compared to assess their effectiveness in MPPT under varying wind conditions.

4.1. Stochastic Wind Speed Profile

In this scenario, we assess the robustness and adaptability of the control strategies in the presence of a stochastic wind speed profile. This profile is characterized by random variations in wind speed over time, representing real-world fluctuations that offshore wind turbines typically encounter. The simulations are conducted over a 100-second duration to observe the controllers' ability to track the MPP and maintain optimal performance. Figure 2 presents the angular speed tracking performance of the three controllers. The FBL controller exhibits a noticeable steady-state error and oscillatory behavior, which indicates suboptimal performance in maintaining the desired speed. The SMC controller, while reducing the steady-state error compared to FBL, introduces chattering, as evident from the oscillations around the reference speed. In contrast, the IBRTA controller significantly outperforms both SMC and FBL, displaying minimal steady-state error and faster convergence, as highlighted in the zoomed section of Figure caption

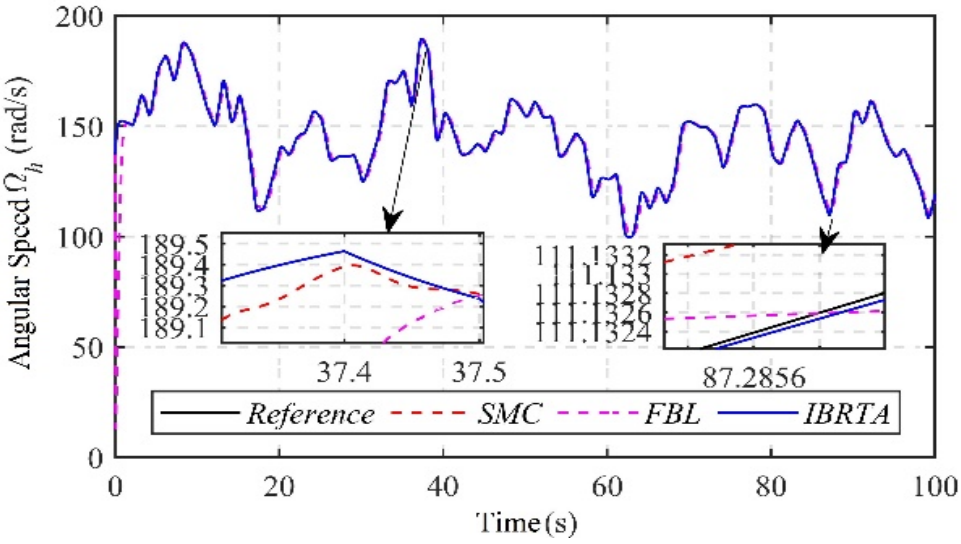

Figure 2. Desired and actual angular speed

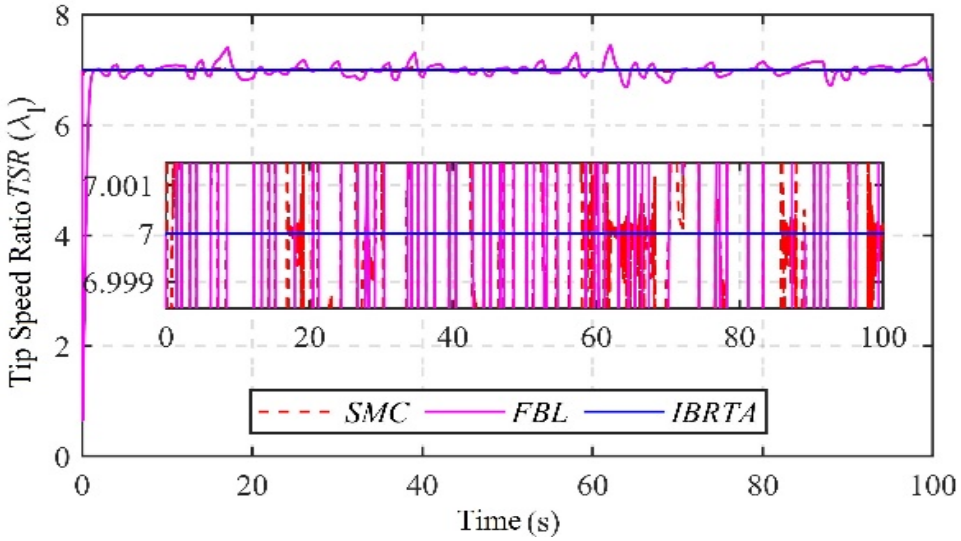

Figure 3. Tip speed ratio versus time plot.

Further analysis is provided in Figures 3 and 4, where the IBRTA controller demonstrates superior performance in maintaining the tip-speed ratio (TSR) and turbine power coefficient (C_{pr}) within optimal ranges. This indicates that the IBRTA controller is more effective in achieving MPPT under stochastic wind conditions compared to SMC and FBL. Additionally, Figure 5 shows that IBRTA and SMC both outperform FBL in maintaining the mechanical power of the turbine shaft within the optimal range, confirming the elimination of chattering by the IBRTA strategy.

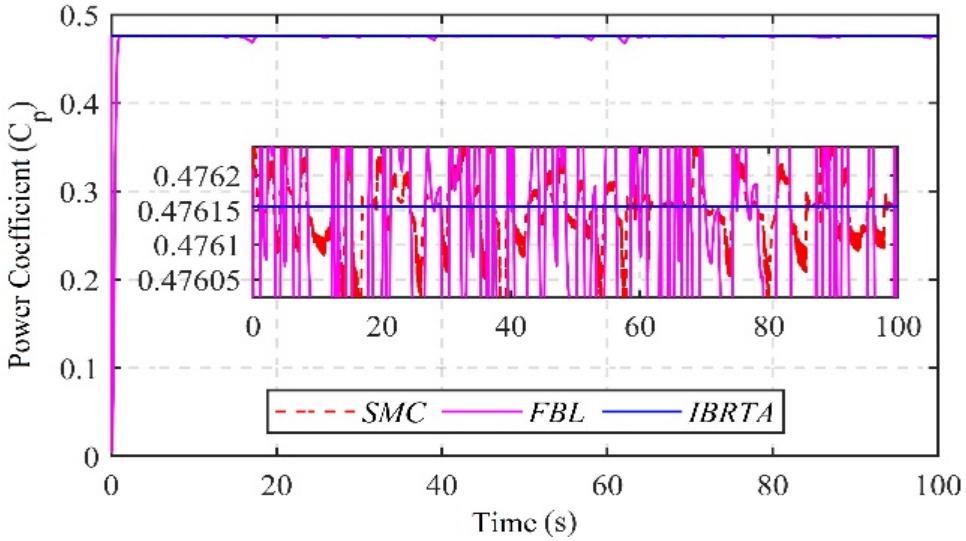

Figure 4. Turbine power coefficient over time

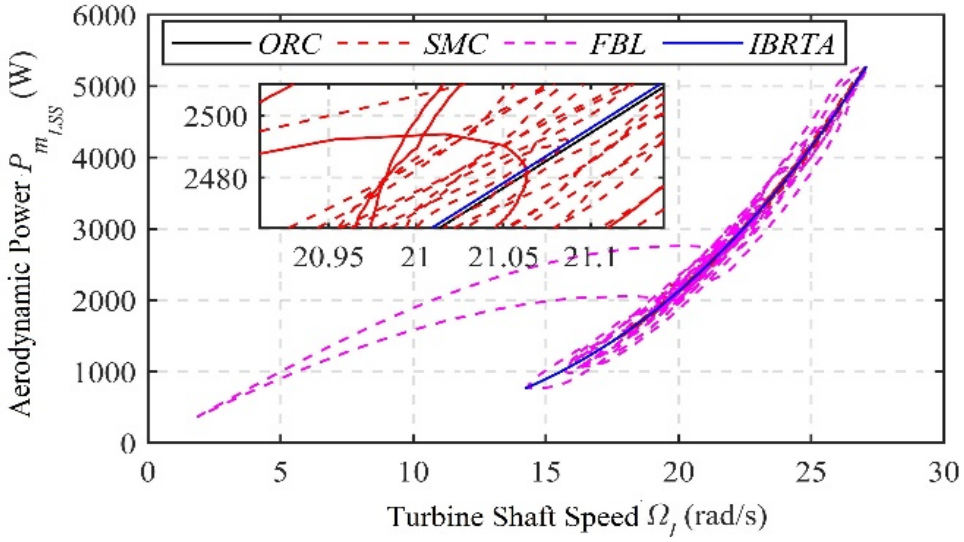

Figure 5. Turbine shaft speed as a function of aerodynamic power

The results from this scenario suggest that the IBRTA controller offers significant improvements in steady-state accuracy and response time over the SMC and FBL controllers, making it the preferred choice for handling the unpredictability of offshore wind conditions.

4.2. *Deterministic Offshore Wind Speed Profile*

In this case study, the controllers' performance is evaluated using a deterministic offshore wind speed profile characterized by abrupt and significant fluctuations in wind velocity.

This scenario aims at assessing the controllers' performance in adjusting the rotor speed as a result of changes in wind speeds while at the same time ensuring maximum power production. As seen from Figure 4.2, all three controllers are able to track the deterministic wind speed profile. The SMC and FBL controllers have oscillations and sudden changes in their output suggesting that they have some challenge in managing the variation in wind speed.

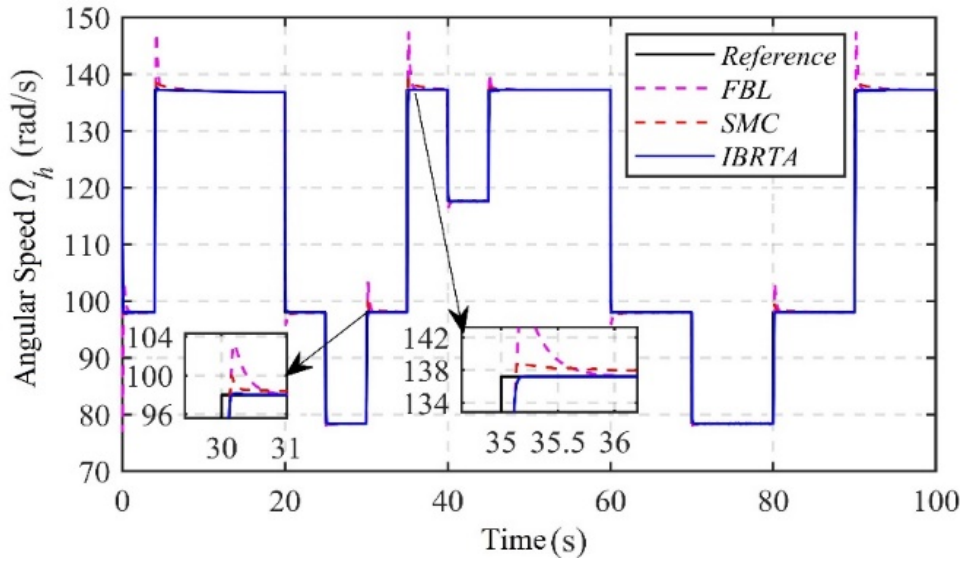

Figure 6: Desired versus actual deterministic speed profile

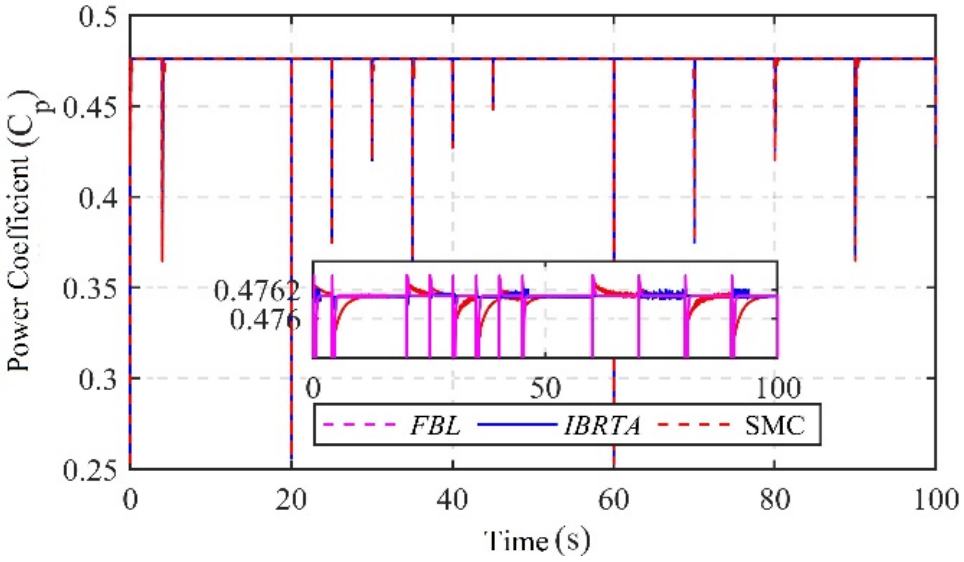

Figure 7. Power coefficient over time

The IBRTA controller, however, shows better performance and stability as compared to the other controller; less oscillation and better tracking of the desired speed. The effectiveness of the IBRTA controller is also emphasized in Figures 7 and 8 where it has a better and smooth power coefficient (C_{pr}) and TSR in the face of the deterministic wind profile. This indicates that the proposed IBRTA controller is capable of tracking the MPPT despite sudden variations in wind speed. Figures 9, 10 shows the power generated and power of the turbine respectively.

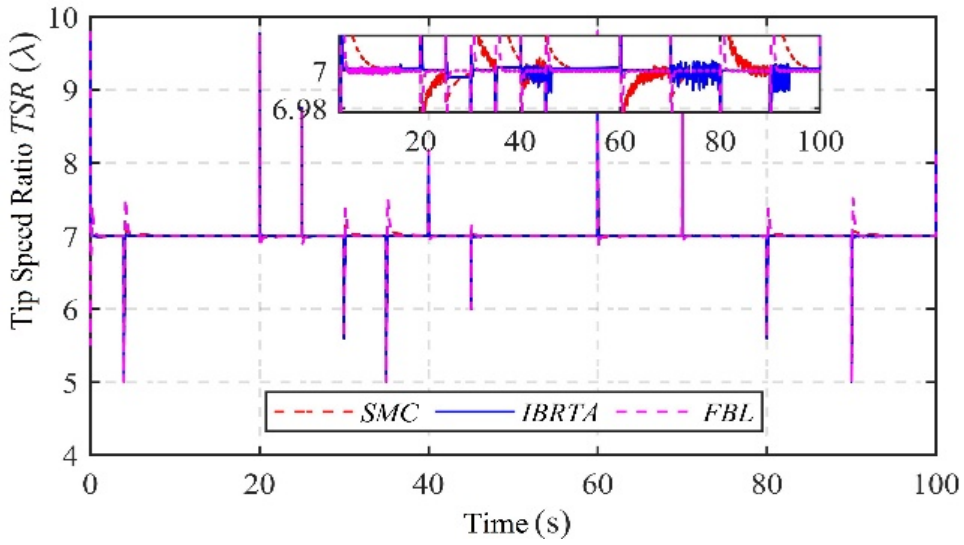

Figure 8. Tip-Speed Ratio over time for the deterministic profile

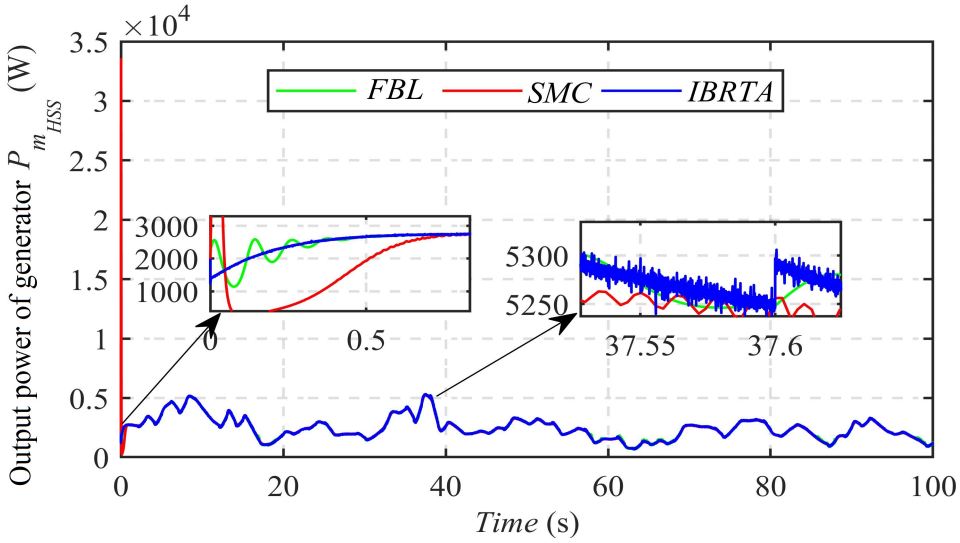

Figure 9. Generated power from the generator

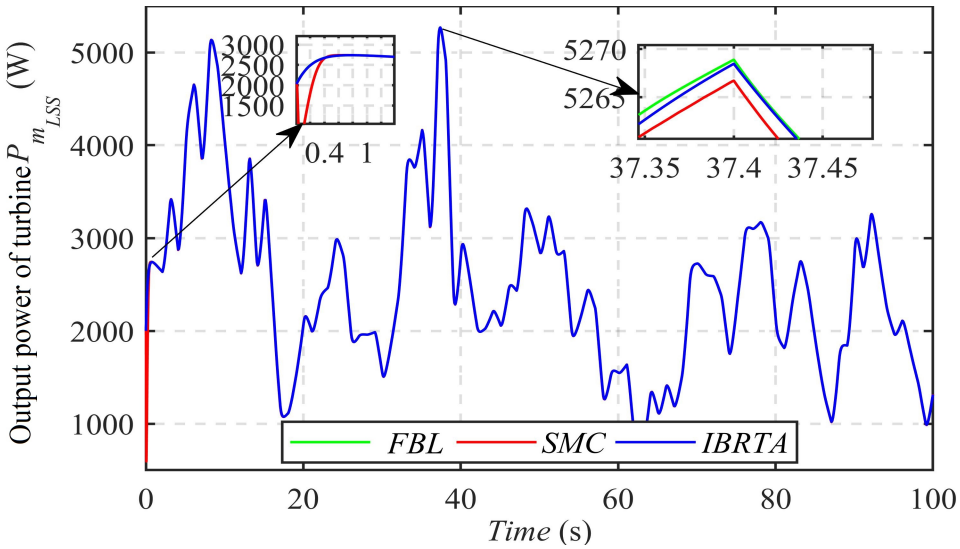

Figure 10. Output power of turbine

4.3. *Discussion and Recommendations*

From the simulation results of both the scenarios, it can be observed that the proposed IBRTA control system outperforms the SMC and FBL controllers in terms of system stability, speed tracking, and power output. The IBRTA controller's steady-state error reduction, chattering reduction, and optimal performance under both stochastic and deterministic wind conditions makes it the best strategy for MPPT in offshore wind energy systems. As for the application, power engineers are encouraged to employ the IBRTA controller most especially when wind conditions are transient or volatile. The proposed IBRTA strategy offers several benefits in terms of energy yield optimization and offshore wind energy system reliability due to its flexibility and resilience.The IBRTA method shows important strengths against the MPPT methods based on machine learning (ML): the predictive features of the data-driven models. However, the IBRTA approach is superior regarding robustness and reliability as show in Figures 9 and 10. The ML approaches often exhibit good performance in the conditions that they are known or trained by, but when tested in an untrained setting, they may underperform, necessitating retraining and large amounts of data. Also, they may be black-boxes, which can impede explanity and respondiveness in real-time. MPPT methods based on adaptive control, in their turn, have

superior parameter tuning capabilities and are capable of withstanding moderate changes in operating conditions. However, they tend to have limits when highly nonlinear time varying or discontinuous dynamics are involved, as is the case in offshore wind systems. In the proposed IBRTA controller, which combines backstepping methodology with robust sliding mode logic, a good compromise between deterministic robustness and smooth adaptive behavior is obtained. It guarantees fast convergence speed, good disturbance rejection, and minimal chattering without the need of any data-driven training. These features enable IBRTA to be a more performance confident and robust solution to maximum power point tracking, particularly in severe and varying environment like that faced in offshore renewable energy systems. Although controller design and initial validation were carried out with MATLAB/Simulink, a tool that is commonly employed in research studies due to its ease of use and flexibility, we recognize that industry-level simulation packages such as OpenFAST or Bladed provide higher fidelity for end-to-end system analysis. The present work concentrates on early-stage validation, with follow-on work expected to include the use of OpenFAST to make the simulations more robust and realistic.

5. CONCLUSIONS

This research proposes a novel system for offshore PMSG based wind energy conversion systems. The model that was initially based on three states is reduced to a two-state normal form with the emphasis on output control. For the purpose of improving the control strategy, SMC is used which allows for appropriate wind speed control across a range of conditions including normal and deterministic offshore wind conditions. Therefore, the proposed MPPT strategy, especially the IBRTA, is evaluated using MATLAB/Simulink. The IBRTA strategy appears to be the most effective strategy among all the discussed strategies as it has potential to offer enhanced efficiency and reliability for offshore wind energy conversion.

Besides, analyzing how the application of artificial intelligence and machine learning could be combined with the IBRTA approach to better address the dynamics of the wind flow could improve the latter even further. For real-world implementation, a pilot experiment of the proposed MPPT control methods must be developed on the basis of factors such as real-time compatibility with embedded processors (e.g., FPGA or DSP), integration of SCADA systems in offshore wind farms without any downtime, and simulation against actual-site wind/load conditions. Safety-centric boundaries such as over-speed protection, hardware redundancy, and protection relays have to be implemented. In addition, performance should be evaluated using quantitative parameters like power capture efficiency, response time, mechanical loading and control stability.

6. References

1. Abdullah, M.A.; Yatim, A.; Tan, C.W.; Saidur, R. A review of maximum power point tracking algorithms for wind energy systems. *Renewable and Sustainable Energy Reviews* **2012**, *16*, 3220–3227.
2. Kazmi, S.M.R.; Goto, H.; Guo, H.J.; Ichinokura, O. Review and critical analysis of the research papers published till date on maximum power point tracking in wind energy conversion system. In *2010 IEEE Energy Conversion Congress and Exposition*; IEEE: 2010; pp. 4075–4082.
3. Mishra, S.; Shukla, S.; Verma, N. Comprehensive review on maximum power point tracking techniques: wind energy. In *2015 Communication, Control and Intelligent Systems (CCIS)*; IEEE: 2015; pp. 464–469.
4. Guimarães, J.S.; de Almeida, B.R.; Tofoli, F.L.; de Souza Oliveira, D. Three-phase grid-connected WECS with mechanical power control. *IEEE Transactions on Sustainable Energy* **2018**, *9*, 1508–1517.
5. Wang, Q.; Chang, L. An intelligent maximum power extraction algorithm for inverter-based variable speed wind turbine systems. *IEEE Transactions on Power Electronics* **2004**, *19*, 1242–1249.
6. Khan, M.A.; Ullah, S.; Khan, L.; Khan, Q.; Khan, Z.A.; Zaman, H.; Ahmad, S. Observer based higher order sliding mode control scheme for PMSG-WECS. In *2019 15th International Conference on Emerging Technologies (ICET)*; IEEE: 2019; pp. 1–6.

7. Dalala, Z.M.; Zahid, Z.U.; Lai, J.-S. New overall control strategy for small-scale WECS in MPPT and stall regions with mode transfer control. *IEEE Transactions on Energy Conversion* **2013**, *28*, 1082–1092.
8. Wei, C.; Zhang, Z.; Qiao, W.; Qu, L. An adaptive network-based reinforcement learning method for MPPT control of PMSG wind energy conversion systems. *IEEE Transactions on Power Electronics* **2016**, *31*, 7837–7848.
9. Barakati, S.M.; Kazerani, M.; Aplevich, J.D. Maximum power tracking control for a wind turbine system including a matrix converter. *IEEE Transactions on Energy Conversion* **2009**, *24*, 705–713.
10. Simoes, M.; Bose, B.K.; Spiegel, R.J. Design and performance evaluation of a fuzzy-logic-based variable-speed wind generation system. *IEEE Transactions on Industry Applications* **1997**, *33*, 956–965.
11. Pucci, M.; Cirrincione, M. Neural MPPT control of wind generators with induction machines without speed sensors. *IEEE Transactions on Industrial Electronics* **2010**, *58*, 37–47.
12. Khan, M.A.; Khan, Q.; Khan, L.; Khan, I.; Alahmadi, A.A.; Ullah, N. Robust differentiator-based NeuroFuzzy sliding mode control strategies for PMSG-WECS. *Energies* **2022**, *15*, 7039.
13. Soufi, Y.; Kahla, S.; Bechouat, M. Feedback linearization control based particle swarm optimization for maximum power point tracking of wind turbine equipped by PMSG connected to the grid. *International Journal of Hydrogen Energy* **2016**, *41*, 20950–20955.
14. Lu, X.-Y.; Spurgeon, S.K. Output feedback stabilization of MIMO non-linear systems via dynamic sliding mode. *International Journal of Robust and Nonlinear Control* **1999**, *9*, 275–305.
15. Ayub, M.W.; Ma, X. Nonlinear super-twisting based speed control of PMSG-ECS using higher order sliding mode control. In 2021 26th International Conference on Automation and Computing (ICAC); IEEE: 2021; pp. 1–6.
16. Le, Xuan Chau ; Minh Quan Duong; and Kim Hung Le. Review of the modern maximum power tracking algorithms for permanent magnet synchronous generator of wind power conversion systems. *Energies* **2022**, *16*, 420.
17. Ayub, M.W.; Ma, X. Integration of hybrid offshore wind and wave energy using PMSG and linear generators. In 2023 28th International Conference on Automation and Computing (ICAC)*; IEEE: 2023; pp. 01–06.
18. Khan, I.U.; Khan, L.; Khan, Q.; Ullah, S.; Khan, U.; Ahmad, S. Neuro-adaptive backstepping integral sliding mode control design for nonlinear wind energy conversion system. *Turkish Journal of Electrical Engineering and Computer Sciences* **2021**, *29*, 531–547.
19. Mat-Noh, M.; Arshad, M.R.; Mohd-Mokhtar, R.; Khan, Q. Back-stepping integral sliding mode control (BISMC) application in a nonlinear autonomous underwater glider. In *2017 IEEE 7th International Conference on Underwater System Technology: Theory and Applications (USYS)*; IEEE: 2017; pp. 1–6.
20. Khan, Q.; Bhatti, A.I.; Iqbal, S.; Iqbal, M. Dynamic integral sliding mode for MIMO uncertain nonlinear systems. *International Journal of Control, Automation and Systems* **2011**, *9*, 151–160.